J. Eng. Technol. Sci., Vol. 54, No. 2, 2022, 220209

A New Mechanical Analysis of a Crankshaft-connecting Rod Dynamics Using Lagrange's Trigonometric Identities

Hasan H. Ali[1, *], Firas M. Abdulsattar[2] & Ahmed W. Mustafa[3]

[1]Directorate of Reconstruction and Projects, Ministry of Higher Education and Scientific Research, Baghdad, Iraq
[2]Department of Refrigeration and Air Conditioning Techniques Engineering, Dijlah University College, Baghdad, Iraq
[3]Department of Mechanical Engineering, Al-Nahrain University, Baghdad, Iraq
*E-mail: hha2mf@mail.missouri.edu

Highlights:

- Lagrange's trigonometric identities were used to simplify an actual and an equivalent connecting rod by minimizing the problem to an algebraic form with good accuracy.
- The largest external forces resultant acting in the x-direction was exerted by the single-cylinder engine, while the smallest external forces resultant acting in the x-direction was exerted by the six-cylinder engine in the studied cases.
- The largest resultant of torque imbalance acting on the crankshaft was found to be associated with two-cylinders engines and was negligible for engines with 5 and 6 cylinders.
- The external forces resultant acting in the x-direction and the torque imbalance acting on the crankshaft can be eliminated by using a seven- or more cylinder engine.
- The results also revealed that the values of all external forces resultants acting in the y-direction were equal to zero for multi-cylinder engines.

Abstract: The main objective of this study was to conduct a new and simple but accurate analysis of the dynamics of a crankshaft-connecting rod system based on Lagrange's trigonometric identities. Actual and equivalent connecting rod mass approximations of single- and multi-cylinder reciprocating engines were studied. Several examples were studied to demonstrate the dynamics of the system. Lagrange's trigonometric identities were used to simplify the model, while MATLAB was used to obtain the results. For both the proposed reduced model and the full model, the resultant forces and torques of an actual and an equivalent connecting rod mass were compared. The results showed that the proposed reduced model gives force and torque results that match the results of the full model very well. It was shown that the largest torque imbalance resultant on the crankshaft was exerted by the two-cylinder engine. In addition, it was shown that the largest external forces resultant acting in the x-direction was exerted by the one-cylinder engine. The results also revealed that the resultant of external forces acting in the y-direction was zero for multi-cylinder engines. The relative error, which mainly occurred at the points of maximum force and torque, ranged from about 1% to about 15%.

Keywords: *crankshaft; dynamics; equivalent mass; internal combustion engine; Lagrange's trigonometric identities; torque imbalance*.

Received November 25th, 2020, Revised August 12th, 2021, Accepted for publication December 12th, 2021.
 ISSN: 2337-5779,
DOI: 10.5614/j.eng.technol.sci.2022.54.2.9

1 Introduction

Crankshaft-connection rod mechanisms have many industrial applications, for example in internal combustion engines (ICEs). The dynamics of the crankshaft-connection rod system play a crucial role in the design process of these systems. It is necessary for the designer of an ICE to know the values of the resultants of the forces and torques acting in the engine and how they affect the cycle of operation. Single- and multi-cylinder reciprocating ICEs are widely used to generate power in numerous different mechanical applications, such as power generation stations and automobiles [1]. Inertia forces that are unbalanced in IC engines lead to stresses and torques, which further leads to operation complications. For the purpose of unbalance reduction, the inertia forces and torques of the multi-cylinder reciprocating engine were analyzed for different cylinder configurations.

As balancing an inline internal combustion engine is a very complex problem, these engines have been the subject of a considerable amount of research in the past few decades [2-4]. The analysis of the dynamics of a multi-cylinder reciprocating engine is difficult due to the presence of two motions of the connecting rod mass (translation and rotation). Therefore, most previous works on multi-cylinder reciprocating engines used approximations. The inertia forces due to the connecting rod mass are divided into two parts, at the crankpin (A) and the wrist pin (B), to simplify the analysis [5]. Another simplified method assumes the inertia forces due to the crankshaft in the crankpin (A), while the connecting rod mass is also divided into two parts: crankpin (A) and wrist pin (B) [6]. These methods clearly do not reflect an exact mathematical model of the multi-cylinder reciprocating engine.

In Koizumi, *et al.* [7], a new analytical model for the purpose of predicting the secondary motion of the piston as well as the vibration that results from the slap of the piston was derived and different engine models were studied. In Hassan [8], the results from numerical investigations of the force of the side thrust, which leads to linear wear, as well as the inertial torque imbalance are presented. Four cases were studied in the analysis of the dynamics of a multi-cylinder reciprocating engine. A design concept that allows for the compensation of the force of simultaneous shaking, the moment of shaking balancing, and the inertial torque imbalance in internal combustion engines is described in Arakelian & Briot [9]. A mathematical model in which the finite element method was used for determining the torque imbalance by reducing the maximum change in engine speed, which leads to excessive crankshaft torsional vibrations in inline six-piston engines, is presented in Gupta, *et. al.* [10]. A numerical example found out by using the ADAMS software was given along with the suggested solution.

A complete analysis of the kinematic and combined static and reaction force of an inline one-piston in a four-stroke reciprocating engine is presented in Desai [11]. The Fortran programing language was used for the analytical approach, as it is less time-consuming and has high accuracy. In Essienubong & Bismarck [12], the piston assembly of an engine under conditions of a typical IC engine was modeled. The finite element method was used and a simulation was performed to determine the effects of the heat and forces exerted on the piston that result from fuel combustion. The results showed that an increase in piston reciprocating leads to an increase in the torque transmitted to the crankshaft. Guan, *et al.* [13] developed nonlinear kinematic constraint equations using a generalized computational method for spatial kinematic analysis of a spherical pump to investigate the displacement, velocity, and acceleration characteristics. The above parameters were investigated for an axial piston pump by Shen, *et al.* [14] using a virtual prototyping approach to analyze both the kinematics and the dynamics. Guan, *et al.* [15] established kinematic constraint models of a robot excavator for pile construction, where the model was used to eliminate the contact between the robot excavator and the pile shaft.

In this work, a new and simple but accurate model for crankshaft-connecting rod mechanisms that may be used in ICEs was tested. There are three inertia forces in the center of the body: the inertia force resulted from the weight of the piston assembly, the inertia force due to the connecting rod, and the inertia force due to the crank. A new approximation of modeling the inertia forces and torques of ICEs by using Lagrange's trigonometric identities for the cases of actual and equivalent mass approximations is proposed. The results of the actual and the proposed model were compared. The resulting outcomes can be used as guidelines to use Lagrange's trigonometric identities with equivalent mass to model the inertia forces and torques in ICEs. The results for the actual and the equivalent mass of the connected rod were in terms of the resultants of all external forces applied in the x-direction and y-direction, and the torque exerted on the crank.

2 System Descriptions

In Figure 1, a schematic of the slider-crankshaft mechanism of an internal combustion engine is shown. It is a classical four-bar slider-crankshaft mechanism that is used in many engineering applications. In the figure, the crankshaft is represented by the symbol r and its mass center is represented by r_1. In addition, the symbol R represents the connecting rod, whose center of mass is represented by the symbol R_1. The piston of the IC engine is represented by a square box that is allowed to move linearly.

The piston center locates the center of mass of the piston relative to the connecting rod pin joint. Rotation of the crankshaft in the direction determined by angle α leads to a back and forth linear piston movement, which changes the piston's position x. During the motion of the crankshaft, the connecting rod's angular position β keeps changing across the piston centerline for the case where $R >> r$. The symbol T in Figure 1 represents the braking torque with respect to the *z*-axis that the crankshaft is subjected to, for a single-piston IC engine. In Figure 1, the crankshaft mass, connecting rod mass, and piston mass are represented by the symbols m_r, m_d, and m_p respectively. The crankshaft's and connecting rod's mass moments-of-inertia about their center of mass are represented by the symbols I_r and I_d, respectively.

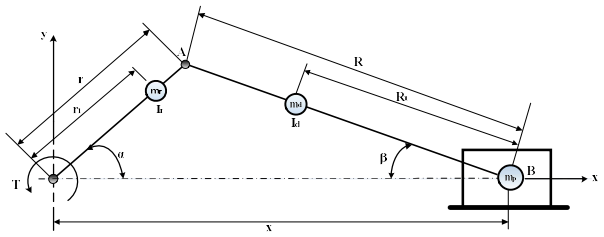

Figure 1 Schematic of the slider-crankshaft mechanism of the actual connecting rod.

3 Modeling and Analysis

Kinematic and kinetic analysis were used to model the inertia forces and torque associated with the operation of the system illustrated in Figure 1.

3.1 Kinematic Modeling and Analysis

Based on Fig. 1, the loop-closure method can be used for the description of the linkage positions, velocity, and acceleration of the piston during its reciprocating within the IC engine. The instantaneous positions of the linkage are:

$$x = r\cos(\alpha) + R\cos(\beta) \quad \text{and} \quad \sin(\beta) = \frac{r}{R}\sin(\alpha) \tag{1}$$

where r is the crankshaft length, R is the connecting rod length, α and β are the angular positions of the crankshaft and the connecting rod, respectively. Assuming angle α is known, Eq. (1) can be solved to determine x and β. In a

similar manner, the velocities of the linkage can be determined from the following equations:

$$\dot{x} = -r\sin(\alpha)\,\dot{\alpha} + R\sin(\beta)\,\dot{\beta} \quad \text{and} \quad 0 = r\cos(\alpha)\,\dot{\alpha} - R\cos(\beta)\,\dot{\beta} \tag{2}$$

Solving the above equations gives the piston velocity, $\dot{x}$, and the connecting rod angular velocity, $\dot{\beta}$,

$$\dot{x} = -r\frac{\sin(\alpha-\beta)}{\cos(\beta)}\dot{\alpha} \quad \text{and} \quad \dot{\beta} = \frac{r}{R}\frac{\cos(\alpha)}{\cos(\beta)}\dot{\alpha} \tag{3}$$

The solution for β, upon which the results of Eq. (3) depend, can be determined using Eq. (1), assuming that the crankshaft angular position and velocity (α and $\dot{\alpha}$) are known. The accelerations of the linkage may be described as follows:

$$\begin{aligned} \ddot{x} &= -r\sin(\alpha)\,\ddot{\alpha} - \alpha\cos(\alpha)\,\dot{\alpha}^2 + R\sin(\beta)\,\ddot{\beta} + R\cos(\beta)\,\dot{\beta}^2 \\ &\text{and} \\ 0 &= r\cos(\alpha)\,\ddot{\alpha} - \alpha\sin(\alpha)\,\dot{\alpha}^2 - R\cos(\beta)\,\ddot{\beta} + R\sin(\beta)\,\dot{\beta}^2 \end{aligned} \tag{4}$$

Solving these equations simultaneously gives the following results for the piston linear acceleration, $\ddot{x}$, and the connecting rod angular acceleration, $\ddot{\beta}$,

$$\begin{aligned} \ddot{x} &= -\alpha\cos(\alpha)\,\dot{\alpha}^2 + R\sin(\beta)\,\ddot{\beta} + R\cos(\beta)\,\dot{\beta}^2 \\ \ddot{\beta} &= \frac{r^2}{R^2}\frac{\cos^2(\alpha)}{\cos^2(\beta)}\tan(\beta)\dot{\alpha}^2 - \frac{r}{R}\frac{\sin(\alpha)}{\cos(\beta)}\dot{\alpha}^2 \end{aligned} \tag{5}$$

These results will be used later in the dynamics analysis of the mechanism.

3.2 Kinetics Modeling and Analysis

For the purpose of performing the slider-crankshaft mechanism kinetics analysis, the coordinate axes *x* and *y* are determined as shown in Figure 1. The resultant of all external forces and torques acting on the slider-crankshaft mechanism will be completely defined by its components in the x- and y-directions, $\sum F_x$ and $\sum F_y$, respectively, and the torque, T, with respect to the z-axis. To find these forces and torques when the motion of the slider-crankshaft mechanism is known, the linear and angular momentum principle is useful. Using the linear and angular momentum principle in the x-direction for the slider-crankshaft mechanism produces the following equations of motion:

$$\sum F_x = \frac{d}{dt}\left(m_r r_1\dot{\alpha}\sin(\alpha) + m_d R_1\dot{\beta}\sin(\beta) - m_p\dot{x}\right) \tag{6}$$

From which,

$$\sum F_x = m_r r_1 \dot{\alpha}^2 \cos(\alpha) + m_r r_1 \ddot{\alpha} \sin(\alpha) + m_d R_1 \dot{\beta}^2 \cos(\beta) + m_d R_1 \ddot{\beta} \sin(\beta) - m_p \ddot{x} \tag{7}$$

where r_1 is the crankshaft mass center, R_1 is the connecting rod center of mass, where m_r, m_d, m_p are the crankshaft mass, connecting rod mass, and piston mass, respectively. Substituting Eqs. (1), (3) and (5) into Eq. (7) gives,

$$\begin{aligned}\sum F_x = {} & \left(m_r r_1 + m_p r\right)\cos(\alpha)\dot{\alpha}^2 + m_r r_1 \sin(\alpha)\ddot{\alpha} + \left(m_d R_1 + m_p R\right)\frac{r^2}{R^2} \\ & \frac{\cos^2(\alpha)}{\cos(\beta)}\left(1+\tan^2(\beta)\right)\dot{\alpha}^2 - \left(m_d R_1 + m_p R\right)\frac{r}{R}\tan(\beta)\sin(\alpha)\dot{\alpha}^2\end{aligned} \tag{8}$$

Similarly, the linear and angular momentum principle in the y-axis for the slider-crankshaft mechanism can be used to produce the following equations of motion:

$$\sum F_y = \frac{d}{dt}\left(-m_r r_1 \dot{\alpha}\cos(\alpha) - m_d R_1 \dot{\beta}\cos(\beta)\right) \tag{9}$$

From which,

$$\sum F_y = m_r r_1 \dot{\alpha}^2 \sin(\alpha) - m_r r_1 \ddot{\alpha}\cos(\alpha) + m_d R_1 \dot{\beta}^2 \sin(\beta) - m_d R_1 \ddot{\beta}\cos(\beta) \tag{10}$$

Substituting Eqs. (1), (3) and (5) into Eq. (10) gives,

$$\sum F_y = \left(m_r r_1 + m_d \frac{R_1 r}{R}\right)\sin(\alpha)\dot{\alpha}^2 - m_r r_1 \cos(\alpha)\ddot{\alpha} \tag{11}$$

Using the previous equations, the torque may be written as,

$$T = -\sum F_x r \sin\alpha + \sum F_y r \cos\alpha \tag{12}$$

Substitution of Eqs. 10) and (11) into Eq. (12) gives,

$$\begin{aligned}T = {} & \left(m_d \frac{R_1}{R} - m_p\right) r^2 \cos(\alpha)\sin(\alpha)\dot{\alpha}^2 - m_r r_1 r \ddot{\alpha} - \left(m_d R_1 + m_p R\right)\frac{r^3}{R^2}\frac{\cos^2(\alpha)\sin(\alpha)}{\cos(\beta)} \\ & \left(1+\tan^2(\beta)\right)\dot{\alpha}^2 + \left(m_d R_1 + m_p R\right)\frac{r^2}{R}\tan(\beta)\sin^2(\alpha)\dot{\alpha}^2\end{aligned} \tag{13}$$

3.3 Lagrange's Trigonometric Identities

For a multi-piston engine with N piston assemblies, the external forces resultant acting on the slider-crankshaft mechanism in the x-direction will be the summation of the reaction forces from each piston assembly. Using Eq. (8), it may be shown that the resultant of the external forces acting on the slider-crankshaft mechanism in the x-direction is given by:

$$\begin{aligned}\sum F_{xt} &= \left(m_r r_1 + m_p r\right)\sum_{n=1}^{N}\cos(\alpha_n)\dot{\alpha}_n^{\,2} + m_r r\sum_{n=1}^{N}\sin(\alpha_n)\ddot{\alpha}_n + \left(m_d R_1 + m_p R\right)\frac{r^2}{R^2} \\ &\sum_{n=1}^{N}\frac{\cos^2(\alpha_n)}{\cos(\beta_n)}\left(1+\tan^2(\beta_n)\right)\dot{\alpha}_n^{\,2} - \left(m_d R_1 + m_p R\right)\frac{r}{R}\sum_{n=1}^{N}\sin(\alpha_n)\ \tan(\beta_n)\dot{\alpha}_n^{\,2}\end{aligned} \tag{14}$$

where α_n is the angular crankshaft position of the n^{th} piston assembly. Similarly, the external forces resultant exerted on the slider-crankshaft mechanism in the y-direction is given by:

$$\sum F_{yt} = \left(m_r r_1 + m_d\frac{R_1 r}{R}\right)\sum_{n=1}^{N}\sin\left(\alpha_n\right)\dot{\alpha}_n^{\,2} - m_r r_1\sum_{n=1}^{N}\cos\left(\alpha_n\right)\ddot{\alpha}_n \tag{15}$$

Finally, using Eq. (13), it may be shown that the torque on the crankshaft from a single-cylinder engine is given by:

$$\begin{aligned}T_t = &\left(m_d\frac{R_1}{R} - m_p\right)r^2\sum_{n=1}^{N}\cos(\alpha_n)\sin(\alpha_n)\dot{\alpha}_n^2 - m_r r r_1\sum_{n=1}^{N}\sin^2(\alpha_n)\ddot{\alpha}_n \\ &-\left(m_d R_1 + m_p R\right)\frac{r^3}{R^2}\sum_{n=1}^{N}\frac{\cos^2(\alpha_n)\sin(\alpha_n)}{\cos(\beta_n)}\left(1+\tan^2(\beta_n)\right)\dot{\alpha}_n^2 \\ &+\left(m_d R_1 + m_p R\right)\frac{r^2}{R}\sum_{n=1}^{N}\sin^2(\alpha_n)\ \tan(\beta_n)\dot{\alpha}_n^2 - m_r r r_1\sum_{n=1}^{N}\cos^2\left(\alpha_n\right)\ddot{\alpha}_n\end{aligned} \tag{16}$$

The summation terms in these equations are a bit complicated. However, if the connecting rods are attached to the crankshaft in an even circular array about the centerline of the shaft according to the following rule,

$$\alpha_n = \alpha_1 + \frac{2\pi}{N}(n-1) \tag{17}$$

then Lagrange's trigonometric identities may be used to simplify the previous Eqs. (14), (15), and (16). Using these identities with Eq. (17), it may be shown that,

$$\begin{aligned}&\sum_{n=1}^{N}\sin^2(\alpha_n) = \sum_{n=1}^{N}\cos^2(\alpha_n) = \frac{N}{2} \\ &\sum_{n=1}^{N}\sin(\alpha_n) = \sum_{n=1}^{N}\cos(\alpha_n) = \sum_{n=1}^{N}\cos(\alpha_n)\sin(\alpha_n) = \sum_{n=1}^{N}\cos^2(\alpha_n)\sin(\alpha_n) = 0\end{aligned} \tag{18}$$

Obviously, the convergence of these series provides a tremendous simplification of the analysis of the internal combustion engine. Substituting Eq. (18) into the foregoing analysis produces the following results for the external forces resultant acting on the slider-crankshaft mechanism in the x-direction,

$$\sum F_{xt} = \left(m_d R_1 + m_p R\right)\frac{r^2}{R^2}\dot{\alpha}^2 \sum_{n=1}^{N} \frac{\cos^2(\alpha_n)}{\cos(\beta_n)}\left(1+\tan^2(\beta_n)\right) - \left(m_d R_1 + m_p R\right)\frac{r}{R}\dot{\alpha}^2 \sum_{n=1}^{N} \sin(\alpha_n)\ \tan(\beta_n) \tag{19}$$

Similarly, substituting Eq. (18) into the foregoing analysis yields the following results for the external forces resultant acting on the slider-crankshaft mechanism in the y-direction:

$$\sum F_{t_y} = 0 \tag{20}$$

Finally, substituting Eq. (18) into the foregoing analysis yields the following results for the torque acting on the slider-crankshaft mechanism:

$$T_t = -m_r r r_1 N \ddot{\alpha}_n - \left(m_d R_1 + m_p R\right)\frac{r^3}{R^2}\sum_{n=1}^{N} \frac{\cos^2(\alpha_n)\sin(\alpha_n)}{\cos(\beta_n)}\left(1+\tan^2(\beta_n)\right)\dot{\alpha}_n^2 + \left(m_d R_1 + m_p R\right)\frac{r^2}{R}\dot{\alpha}^2 \sum_{n=1}^{N} \sin^2(\alpha_n)\ \tan(\beta_n)\dot{\alpha}_n^2 \tag{21}$$

It is clear from these results that Lagrange's trigonometric identities greatly simplify the analysis of the crankshaft-connecting rod dynamics used in ICEs with connecting rods that are spaced about the crankshaft centerline evenly, as shown in Eq. (17).

3.4 Dimensionless Analysis

Dimensionless analysis gives the model generalization to be applied for systems with different sizes and characteristics in addition to reducing the number of parameters in the analysis, as in Ali, *et al.* [16] and Ali [17]. In order to express the previous equation in dimensionless form, the following definitions should be used:

$$R = r\hat{R},\ R_1 = r\hat{R}_1, r_1 = r\hat{r}_1,\ m_d = m_P\hat{m}_d,\ m_r = m_P\hat{m}_r,\ \sum F_x = m_p r\alpha^2 \sum \hat{F}_x,\ \sum F_y = m_p r\alpha^2 \sum \hat{F}_y,\ T = m_p r^2\alpha^2\hat{T},\ \sum F_{xt} = m_p r\alpha^2 \sum \hat{F}_{xt},\ \sum F_{yt} = m_p r\alpha^2 \sum \hat{F}_{yt},\ T_t = m_p r^2\alpha^2\hat{T}_t \tag{22}$$

3.5 Dimensionless Analysis for Single-Cylinder Engine

Using the definitions given in Eqs. (8), (11), and (13), it may be shown that the dimensionless actual external forces resultant and the torque acting on the crankshaft are given by Eqs. (23-25), assuming that the angular velocity of the crankshaft is constant:

$$\sum \hat{F}_x = \left(\hat{m}_r \hat{r}_1 + 1\right)\cos\left(\alpha\right) + \left(\hat{m}_d \hat{R}_1 + \hat{R}\right)\frac{1}{\hat{R}^2}\frac{\cos^2(\alpha)}{\cos(\beta)}\left(1+\tan^2(\beta)\right) - \left(\hat{m}_d \frac{\hat{R}_1}{\hat{R}} + 1\right)\tan(\beta)\sin(\alpha) \tag{23}$$

$$\sum \hat{F}_y = \left(\hat{m}_r \hat{r}_1 + \hat{m}_d \frac{\hat{R}_1}{\hat{R}}\right)\sin\left(\alpha\right) \tag{24}$$

$$\hat{T} = \left(\hat{m}_d \frac{\hat{R}_1}{\hat{R}} - 1\right)\cos\left(\alpha\right)\sin(\alpha) - \left(\hat{m}_d \hat{R}_1 + \hat{R}\right)\frac{1}{\hat{R}^2}\frac{\cos^2(\alpha)\sin(\alpha)}{\cos(\beta)}\left(1+\tan^2(\beta)\right) + \left(\hat{m}_d \hat{R}_1 + \hat{R}\right)\frac{1}{\hat{R}^2}\tan(\beta)\sin^2(\alpha) \tag{25}$$

3.6 Dimensionless Analysis for Multi-Cylinder Engines

Using the definitions with Eq. (19), it may be shown that the dimensionless actual external forces resultant acting in the x-direction is given by,

$$\sum \hat{F}_{xt} = \left(\hat{m}_d \hat{R}_1 + \hat{R}\right)\frac{1}{\hat{R}^2}\sum_{n=1}^{N}\frac{\cos^2(\alpha_n)}{\cos(\beta_n)}\left(1+\tan^2(\beta_n)\right) - \left(\hat{m}_d \frac{\hat{R}_1}{\hat{R}} + 1\right)\sum_{n=1}^{N}\sin(\alpha_n)\ \tan(\beta_n) \tag{26}$$

Similarly, using the definitions in Eq. (21), it may be shown that the dimensionless actual torque acting on the slider-crankshaft mechanism is given by:

$$\hat{T}_t = -\left(\hat{m}_d R_1 + \hat{R}\right)\frac{1}{\hat{R}^2}\sum_{n=1}^{N}\frac{\cos^2(\alpha_n)\sin(\alpha_n)}{\cos(\beta_n)}\left(1+\tan^2(\beta_n)\right) + \left(\hat{m}_d \hat{R}_1 + \hat{R}\right)\frac{1}{\hat{R}^2}\sum_{n=1}^{N}\sin^2(\alpha_n)\ \tan(\beta_n) \tag{27}$$

4 Equivalent Masses of Connecting Rod

In this case, equivalent masses were used to reduce the problem to an algebraic form. The slider-crankshaft mechanism replaces the connecting rod by two equivalent masses, m_A and m_B, at its ends, A and B, as shown in Figure 2.

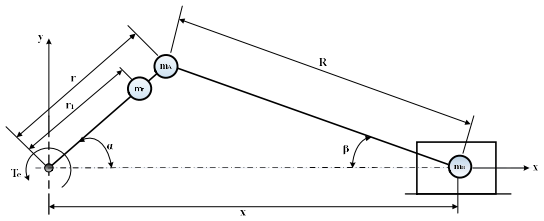

Figure 2 Schematic of the slider-crankshaft mechanism for equivalent masses of the connecting rod.

The summation of these two masses should equal the actual connecting rod mass m_d .

$$m_d = m_A + m_B \tag{28}$$

In addition, their mass centers should coincide with that of the connecting rod,

$$m_A\left(R - R_1\right) = m_B R_1 \tag{29}$$

From Eqs. (28) and (29),

$$m_A = m_d\left(\frac{R_1}{R}\right) \text{ and } m_B = m_d\left(1 - \frac{R_1}{R}\right) \tag{30}$$

At the piston pin, m_B is added to the mass of piston m_p to determine the total joint mass,

$$m = m_p + m_B \tag{31}$$

Applying the linear and angular momentum principle in the x-direction to the slider-crankshaft mechanism for equivalent masses of the connecting rod gives the equations of motion defined in Eq. (32),

$$\sum F_{xe} = \frac{d}{dt}\left(m_r r_1 \dot{\alpha}\sin(\alpha) + m_A r\dot{\alpha}\sin(\alpha) - m\dot{x}\right) \tag{32}$$

From which,

$$\sum F_{xe} = m_r r_1 \dot{\alpha}^2\cos(\alpha) + m_r r_1 \ddot{\alpha}\sin(\alpha) + m_A r\dot{\alpha}^2\cos(\alpha) + m_A r\ddot{\alpha}\sin(\alpha) - m\ddot{x} \tag{33}$$

Substituting Eq. (5) into Eq. (29) gives,

$$\begin{aligned}\sum F_{xe} = {} & \left(m_r r_1 + r\left(m_A + m\right)\right)\cos(\alpha)\dot{\alpha}^2 + \left(m_r r_1 + m_A r\right)\sin(\alpha)\ddot{\alpha} \\ & + m\frac{r^2}{R}\frac{\cos^2(\alpha)}{\cos(\beta)}\left(1 + \tan^2(\beta)\right)\dot{\alpha}^2 - m\, r\tan(\beta)\sin(\alpha)\dot{\alpha}^2\end{aligned} \tag{34}$$

Similarly, the linear and angular momentum principle can be used in the y-direction for the slider-crankshaft mechanism for equivalent connecting rod masses, yielding the following equations of motion:

$$\sum F_{ye} = \frac{d}{dt}\left(-m_r r_1 \dot{\alpha}\cos(\alpha) - m_A r \dot{\alpha}\cos(\alpha)\right) \tag{35}$$

From which,

$$\sum F_{ye} = \left(m_r r_1 + m_A r\right)\left(\dot{\alpha}^2 \sin(\alpha) - \ddot{\alpha}\cos(\alpha)\right) \tag{36}$$

Finally, the equivalent torque exerted on the crankshaft may be determined using the previous equations. The result is given by

$$T_e = -\sum F_{xe}\, r\sin\alpha + \sum F_{ye}\, r\cos\alpha \tag{37}$$

Substituting Eqs. (34) and (36) into Eq. (37) yields

$$\begin{aligned} T_e = {} & mr\cos(\alpha)\sin(\alpha)\dot{\alpha}^2 - r\left(m_r r_1 + m_A r\right)\ddot{\alpha} - m\frac{r^3}{R}\frac{\cos^2(\alpha)\sin(\alpha)}{\cos(\beta)} \\ & \left(1+\tan^2(\beta)\right)\dot{\alpha}^2 + m\, r^2\, \tan(\beta)\sin^2(\alpha)\dot{\alpha}^2 \end{aligned} \tag{38}$$

4.1 Lagrange's Trigonometric Identities

Similar to the development of Eqs. (34), (36), and (38), the equivalent total resultant of all external forces acting in the x-direction and y-direction and the equivalent torque on the slider-crankshaft mechanism with a multi-cylinder engine can be computed by setting $\alpha \to \alpha_n$ and $\beta \to \beta_n$ in Eqs. (34), (36), and (38), where α_n and β_n are defined by Eq. (16). Using these equations, the equivalent total external forces resultant acting in the x-direction and y-direction and the torque on the slider-crankshaft mechanism may be computed as,

$$\sum F_{xet} = m\frac{r^2}{R}\sum_{n=1}^{N}\frac{\cos^2(\alpha_n)}{\cos(\beta_n)}\left(1+\tan^2(\beta_n)\right)\dot{\alpha}_n^{\,2} - mr\sum_{n=1}^{N}\tan(\beta_n)\sin(\alpha_n)\dot{\alpha}_n^{\,2} \tag{38}$$

and

$$\sum F_{yet} = 0 \tag{39}$$

$$T_{et} = -m\frac{r^3}{R}\sum_{n=1}^{N}\frac{\cos^2(\alpha_n)\sin(\alpha_n)}{\cos(\beta_n)}\left(1+\tan^2(\beta_n)\right)\dot{\alpha}_n^{\,2} + mr^2\sum_{n=1}^{N}\sin^2(\alpha_n)\tan(\beta_n)\dot{\alpha}_n^{\,2} \tag{41}$$

4.2 Dimensionless Analysis

In order to express Eq. (34) and (36) in dimensionless form, the following definitions are used:

$$\begin{aligned} &R = r\hat{R},\ R_1 = r\hat{R}_1, r_1 = r\hat{r}_1,\ m_d = m_P\hat{m}_d,\ m_r = m_P\hat{m}_r, \\ &\sum F_{xe} = mr\alpha^2\sum\hat{F}_{xe},\ \sum F_{ye} = m_p r\alpha^2\sum\hat{F}_{ye},\quad T_e = mr^2\alpha^2\hat{T}_e, \\ &\sum F_{xet} = mr\alpha^2\sum\hat{F}_{xet},\ \sum F_{yet} = m_p r\alpha^2\sum\hat{F}_{yet},\ T_{et} = mr^2\alpha^2\hat{T}_{et} \end{aligned} \tag{42}$$

4.3 Dimensionless Analysis for Single-Cylinder Engine

Using the definitions with Eq. (34), (36), and (38), it may be shown that the dimensionless equivalent external forces resultant and the torque exerted on the crankshaft are given by assuming that the angular velocity of the crankshaft is constant:

$$\sum\hat{F}_{xe} = \left(\hat{m}_r\hat{r} + \hat{m}_A + 1\right)\cos(\alpha) + \frac{1}{\hat{R}}\frac{\cos^2(\alpha)}{\cos(\beta)}\left(1+\tan^2(\beta)\right) - \tan(\beta)\sin(\alpha) \tag{43}$$

$$\sum\hat{F}_{ye} = \left(\hat{m}_r\hat{r}_1 + \hat{m}_A\right)\sin(\alpha) \tag{44}$$

$$\hat{T}_e = -\cos(\alpha)\sin(\alpha) - \frac{1}{\hat{R}}\frac{\cos^2(\alpha)\sin(\alpha)}{\cos(\beta)}\left(1+\tan^2(\beta)\right) + \tan(\beta)\sin^2(\alpha) \tag{45}$$

Eqs. (43), (44), and (45) are the reduced forms of Eqs. (23), (24), and (25), respectively.

4.4 Dimensionless Analysis for Multi-Cylinder Engine

Using the definitions given in Eqs. (39) and (41), it may be shown that the dimensionless equivalent external forces resultant and the torque exerted on the crankshaft are given by

$$\sum\hat{F}_{xet} = \frac{1}{\hat{R}}\sum_{n=1}^{N}\frac{\cos^2(\alpha_n)}{\cos(\beta_n)}\left(1+\tan^2(\beta_n)\right) - \sum_{n=1}^{N}\tan(\beta_n)\sin(\alpha_n) \tag{40}$$

$$\hat{T}_{et} = -\frac{1}{\hat{R}}\sum_{n=1}^{N}\frac{\cos^2(\alpha_n)\sin(\alpha_n)}{\cos(\beta_n)}\left(1+\tan^2(\beta_n)\right) + \sum_{n=1}^{N}\sin^2(\alpha_n)\tan(\beta_n) \tag{41}$$

Eqs. (46) and (47) are the reduced forms of Eqs. (26) and (27), respectively.

5 Results and Discussion

5.1 Resultants of All External Forces Exerted in the X-Direction

The results of the external forces resultant acting in the x-direction of the actual and the equivalent connecting rod are shown below. Lagrange's trigonometric identities were used to simplify the analysis that is presented in this paper for the actual and the equivalent connecting rod mass. Eq. (23) was used to calculate the dimensionless external forces resultant acting in the x-direction of a single-piston engine. The design parameters were assumed for calculation purposes. The results are indicated by the solid line in Figure 3 for one revolution of a one-piston ICE. The equivalent result of Eq. (43) is shown by the dashed line, which matches the results of the actual mass very well.

In many applications, multiple pistons are used in the same ICE. The resultant of external forces acting in the x-direction for these IC engines can be determined using Eq. (26) for the actual connecting rod, while Eq. (46) is used for the equivalent mass connecting rod.

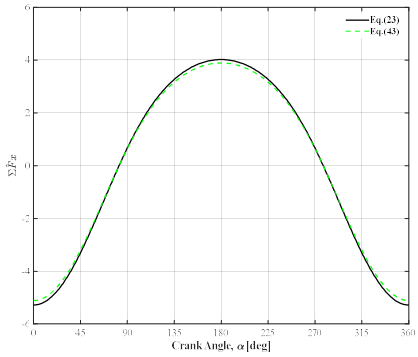

Figure 3 Dimensionless external forces resultant acting in the x-direction of a single-piston engine.

Figure 4 show the results for multi-cylinder engines (N = 2, 3, 4, 5, and 6, respectively). From these figures, it can be seen that the comparison between the actual and the equivalent resultant of all external forces acting in the x-direction during one revolution of the engine have good agreement. It can be seen that the deviation of the results of the equivalent mass approximation from the actual results increases as the number of pistons increases. However, the difference is seen only in the maximum values of the resultant forces and it is less than 10% in the worst case, which confirms that the model simplification does not affect the accuracy of the model in representing the resultants. In addition, it can be seen

that the largest external forces resultant acting in the x-direction was exerted by the single-cylinder engine.

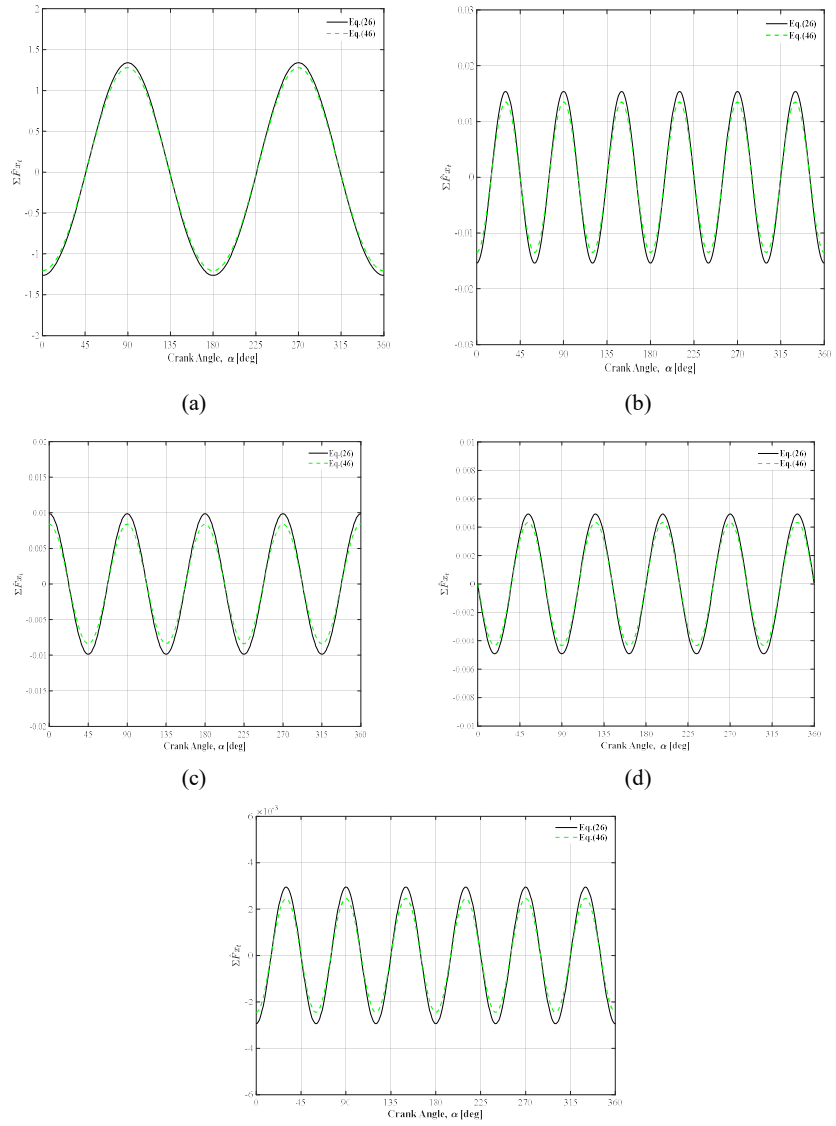

Figure 4 Dimensionless external forces resultant acting in the x-direction of a (a) two-, (b) three-, (c) four-, (d) five-, and (e) six-piston engine.

5.2 External Forces Resultant Acting in the Y-Direction

Figure 5 represents the external forces resultant acting in the y-direction for the actual and the equivalent connecting rod mass calculated by Eq. (24) and Eq. (44). Eq. (24) was used to calculate the dimensionless external forces resultant acting in the y-direction of a single-piston engine, which is indicated by the solid line in Figure 5 for one revolution of a one-piston IC engine. The equivalent result of Eq. (44) is shown by the dashed line. As shown in the figure, the external forces resultant acting in the y-direction for the actual and the equivalent connecting rod have good agreement. The external forces resultant acting in the y-direction for the actual and the equivalent connecting rod for multi-cylinder engines is essentially zero.

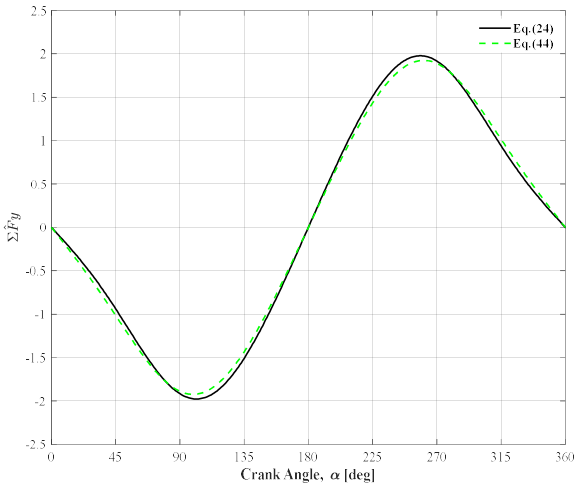

Figure 5 Dimensionless external forces resultant acting in the y-direction of a single-piston engine.

5.3 Torque Acting on the Crankshaft

Figure 6 shows the torque imbalance acting on the crankshaft calculated from Eqs. (25) and (45) for the actual and the equivalent mass connecting rod, respectively, plotted versus crankshaft angle. The result for the actual connecting rod mass is shown by the solid line in Figure 6, while the result for the equivalent mass is illustrated by the dashed line for one revolution of a one-cylinder IC engine. As shown in Figure 6, the actual torque imbalance acting on the crankshaft is very close in magnitude to the equivalent torque acting on the crankshaft, which proves the validity of the simplified model.

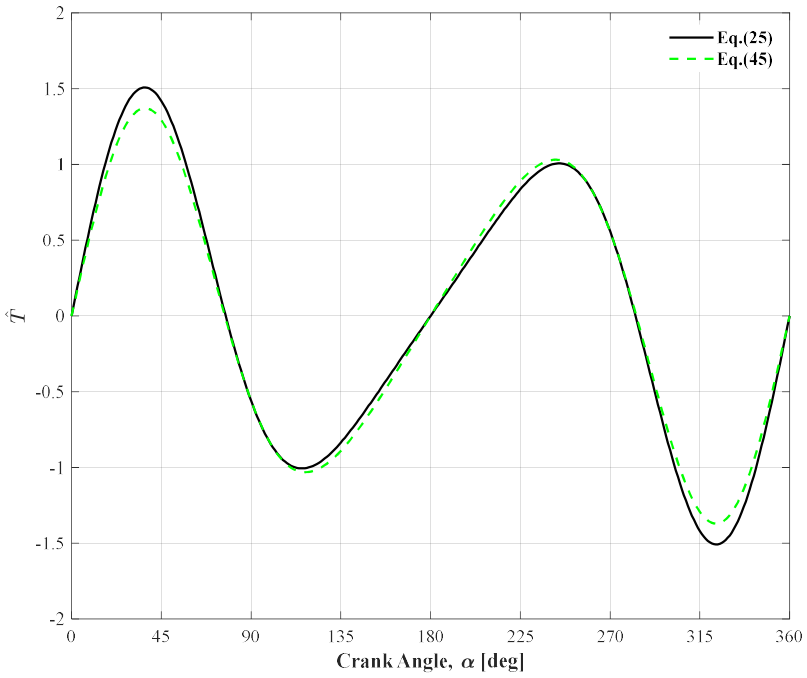

Figure 6 Dimensionless torque exerted on the crankshaft in a one-cylinder engine.

While the one-cylinder engine is of great interest, many engines with a slider-crankshaft mechanism use multiple cylinders in the same engine. The total actual torque exerted on the crankshaft for those engines may be computed using Eq. (27), while the total equivalent torque applied on the crankshaft for these engines may be evaluted using Eq. (47).

Figure 7 shows the results for multi-cylinder engines for the actual and the equivalent connecting rod mass. It can also be seen that the maximum torque imbalance was exerted by the engine with two cylinders. It can be seen that the deviation of the results of the equivalent mass approximation from the actual results increases as the number of pistons increases. However, the difference is seen only in the maximum values of the resultant forces and it is less than 10% in the worst case, which confirms that the model simplification does not affect the accuracy of the model in the representation of those torques. It is worth mentioning that since each engine has cylinder assemblies with the same size, the scale factor which the amplitude requires to be multiplied by for the purpose of determining dimensional torque will not change and is always $mr^2\alpha^2$.

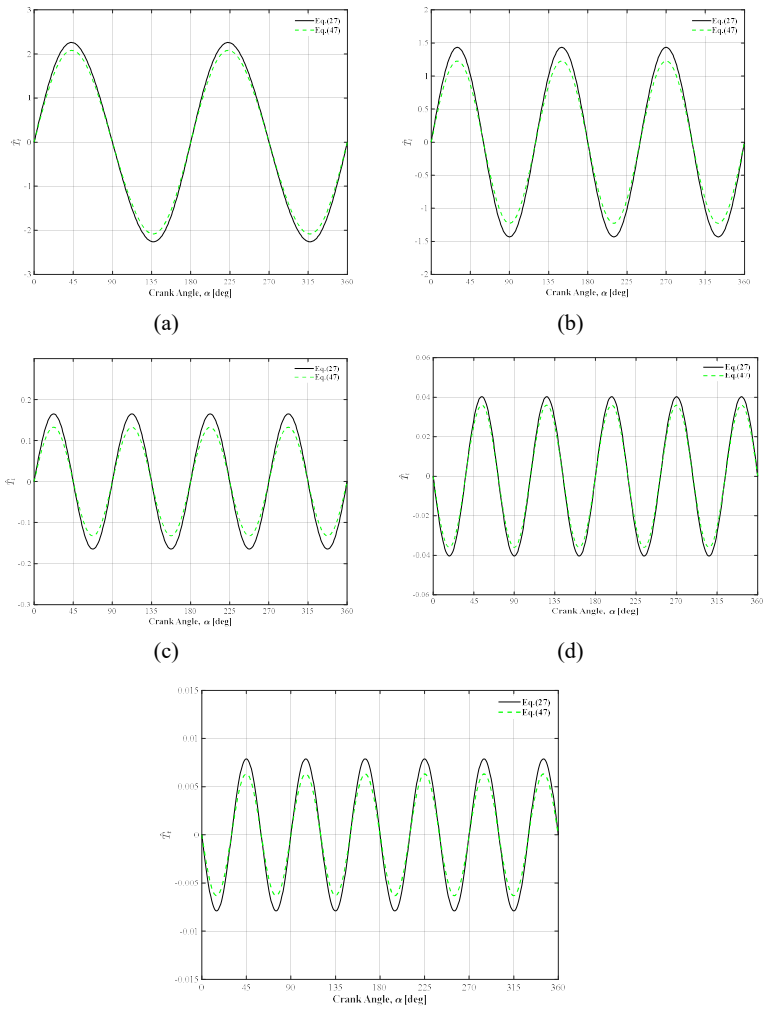

Figure 7 Dimensionless torque applied on the crankshaft in a (a) two-, (b) three-, (c), four-, (d) five-, and (e) six-cylinder IC engine.

6 Conclusions

This paper presented a new way of analyzing and modeling the dynamics of a crankshaft-connecting rod system, which may be used for single- and multi-cylinder reciprocating engines. The ultimate goal of multi-cylinder reciprocating engine analysis is to find an easy procedure that gives accurate solutions because

certain simplifications are used to minimize the problem to an algebraic form for the cases of the actual and the equivalent connecting rod mass. Lagrange's trigonometric identities were used in order to simplify the two cases. The conclusions supported by the results of this paper are:

1. The proposed model based on Lagrange's trigonometric identities provides great simplification to the dynamics of the crankshaft-connecting rod system while keeping good accuracy for actual and equivalent connecting rods by minimizing the problem to an algebraic form.
2. The largest external forces resultant acting in the x-direction is exerted by the single-cylinder engine. The next largest external forces resultant acting in the x-direction is exerted by the two-cylinder engine, followed by the three-cylinder engine, the four-cylinder engine, the five-cylinder engine, and the six-cylinder engine, as shown in Figure 4.
3. The largest resultant of torque imbalance acting on the crankshaft was exerted by the two-cylinder engine. The next largest resultant of torque acting on the crankshaft was exerted by the one-cylinder engine, followed by the three-cylinder engine, the four-cylinder engine, and it is negligible in five- and six-cylinders engines, as shown in Figure 7.
4. The external forces resultant exerted in the x-direction and the torque imbalance exerted on the crankshaft can be eliminated by using seven or more cylinders.
5. The analysis also revealed that the values of all external forces resultants exerted in the y-direction are equal to zero for multi-cylinder engines.

Nomenclature

$\dot{x}$ Instantaneous system velocity in the x-direction
$\dot{y}$ Instantaneous system velocity in the y-direction
$\sum F_x$ The external forces resultant acting in the x-direction
$\sum F_y$ The external forces resultant acting in the y-direction
$\sum F_{xe}$ The resultant of all external forces acting in the x-direction
$\sum F_{ye}$ The resultant of all external forces acting in the y-direction
I_r The crankshaft mass moment of inertia about its mass center
I_d The connecting rod mass moment of inertia about its mass center
r Crankshaft length
R Connecting rod length
m_r Crankshaft mass

m_d	Connecting rod mass
m_p	Piston mass
r_1	Crankshaft mass center location
R_1	Connecting rod mass center location
T_z	Torque exerted on the crankshaft
x	Instantaneous displacement of the piston
α	Crankshaft angular displacement
$\dot{\alpha}$	Crankshaft angular velocity
β	Connecting rod angular displacement of the
$\dot{\beta}$	Connecting rod angular velocity

References

[1] Timoshenko, S. & Young, D. H., *Advanced Dynamics*, McGraw- Hill, New York, New York, 1948.

[2] Manring, N.D. & Dong, Z., *The Impact of Using a Secondary Swash-Plate Angle Within an Axial Piston Pump*, Journal of Dynamic Systems, Measurement, and Control, **126**(1), pp.65-74, 2004.

[3] Kumar, A., *Existing Situation of Municipal Solid Waste Management in NCT Of Delhi*, India. Int. J. Soc. Sci, **1**(1), pp.6-17, 2013.

[4] Hassaan, G.A., *Optimal Kinematic Synthesis of Planar Mechanisms, Part I: Offset Crank-Slider Mechanism*, International Journal of Computer Techniques, **2**(2), pp.151-157, 2015.

[5] Manring, N.D. & Ali, M., *Modeling the Inertial Torque Imbalance within an Internal Combustion Engine: Quantifying the Equivalent Mass Approximation*, Journal of Dynamic Systems, Measurement, and Control, **140**(7), 2018.

[6] Dutta, S. & Naskar, T.K., *Synthesis of Adjustable Offset Slider-Crank Mechanism for Simultaneous Generation of Function and Path using Variable-Length Links*, in Proceedings of the 1st International and 16th National Conference of Machines and Mechanisms, pp. 18-20, 2013.

[7] Koizumi, T., Tsujiuchi, N., Okamura, M., Tsukijima, H., Kubomoto, I. & Ishida, E., *Reduction of Piston Slap Excitation by Optimizing Piston Profiles*, in Proc SPIE Int Soc Opt Eng., pp. 107-113, 2002.

[8] Hassan, T.E., Bilal A. & Gasim, M.M.E., *Theoretical Performance Comparison between Inline, Offset and Twin Crankshaft Internal Combustion Engines*, FES Journal of Engineering Science, **3**(1), pp. 63-79, 2008. DOI: 10.52981/fjes.v3i1.76.

[9] Arakelian, V. & Briot, S., *Simultaneous Inertia Force/Torque Balancing and Torque Compensation of Slider-Crank Mechanisms*, Mechanics Research Communications, **37**(2), pp.265-269, 2010.

[10] Gupta, B.K., Reham, A. & Mittal, N.D., *Validating Experimentally the Gain in Torque due to Crankshaft Offset of Internal Combustion Engine*, Int. J. Eng., **6**(2), pp.76-88, 2014.

[11] Desai, H.D., *Computer Aided Kinematic and Dynamic Analysis of a Horizontal Slider Crank Mechanism Used for Single-Cylinder Four Stroke Internal Combustion Engine*, in Proceedings of the World Congress on Engineering, **2**, pp. 1-3, 2009.

[12] Essienubong, I.A. & Bismarck O.I., *Design Analysis of Reciprocating Piston for Single Cylinder Internal Combustion Engine*, International Journal of Automotive Science and Technology, **4**(2), pp. 30-39, 2020.

[13] Guan, D., Wu, J.H., Jing, L., Hilton, H.H. & Lu, K., *Kinematic Modeling, Analysis and Test on a Quiet Spherical Pump*, J. Sound Vib., **383**, pp. 146-155, 2016.

[14] Shen, H., Zhou, Z., Guan, D., Liu, Z., Jing, L. & Zhang, C., *Dynamic Contact Analysis of The Piston and Slipper Pair in Axial Piston Pump*, Coatings, **10**(12), pp. 1-18, 2020.

[15] Guan, D., Yang, N., Lai, J., Siu, M.-F.F., Jing, X. & Lau, C.K., *Kinematic Modeling and Constraint Analysis for Robotic Excavator Operations in Piling Construction*, Autom. Constr., **126**, 103666, 2021.

[16] Ali, H.H., Fales, R.C. & Manring, N.D. *Modeling and Control Design for an Inlet Metering Valve-Controlled Pump Used to Control Actuator Velocity Via H-Infinity and Two-Degrees-of-Freedom Methods*, ASME. J. Dyn. Sys., Meas., Control. November, **141**(11), 111006, 2019.

[17] Ali, H., *Inlet Metering Pump Analysis and Experimental Evaluation with Application for Flow Control*, Ph.D. Dissertation, University of Missouri-Columbia, 2017.